Available online at www.sciencedirect.com
ScienceDirect
Journal of Nuclear Materials 367–370 (2007) 316–321
journal of nuclear materials
www.elsevier.com/locate/jnucmat

Anisotropy migration of self-point defects in dislocation stress fields in BCC Fe and FCC Cu

A.B. Sivak [a], V.M. Chernov [a,*], N.A. Dubasova [a], V.A. Romanov [b]

[a] *A.A. Bochvar Institute of Inorganic Materials, Rosatom, Moscow, Russia*
[b] *A.I. Leypunskiy Institute of Physics and Power Engineering, Rosatom, Obninsk, Russia*

Abstract

Spatial dependence of the interaction energies of self-point defects (vacancies and self interstitial atoms in stable, metastable and saddle point configurations) with edge dislocations in slip systems $\langle 1\,1\,1\rangle\{1\,1\,0\}$ and $\langle 1\,0\,0\rangle\{1\,0\,0\}$ in BCC Fe and $\langle 1\,1\,0\rangle\{1\,1\,1\}$ in FCC Cu was calculated using the anisotropic theory of elasticity and molecular statics (hybrid method). The migration pathways of vacancies and SIA ($\langle 1\,1\,0\rangle$ dumbbell in Fe and $\langle 1\,0\,0\rangle$ dumbbell in Cu) along which the migration of the defects with the lowest energy barriers were defined in the presence of the dislocation stress fields. These pathways are significantly different in the stress fields of dislocations.

1. Introduction

Stress fields of dislocations, the basic source of internal stresses, considerably effect the kinetic behavior of point defects including their diffusion and absorption by dislocations as sinks. Such processes depend on the symmetry of crystal lattices, elastic anisotropy of crystals and types of crystal defects [1]. It is important to study the influence of dislocation stress fields on formation and migration energies of vacancies and self interstitial atoms (SIA) in crystals of different crystallographic classes.

Here, the spatial dependence of the elastic interaction energy between the self-point defects (SPDs) in stable, metastable and saddle point configurations and straight edge dislocations with different Burgers vectors in BCC Fe and FCC Cu were calculated using a hybrid method. Elastic fields of dislocations and their interactions with SPDs (elastic dipoles) were calculated in the framework of the anisotropic theory of elasticity [2]. Characteristics of SPDs (formation and migration energies, relaxation volumes and dipole moment tensors) in the absence of stress fields were calculated by molecular statics. The influence of these interactions on the migration directions of the SPDs was studied to understand their influence on radiation-induced property changes such as swelling in crystals with different symmetries (BCC, FCC).

2. SPDs characteristics

Formation energies E^{F}, relaxation volumes V^{R}, and dipole tensors P_{ij} ($i,j = 1,2,3$, define the coordinate axes in crystallographic coordinate system) of

* Corresponding author. Tel.: +7 095 1903605; fax: +7 095 1964168.
E-mail address: chernovv@bochvar.ru (V.M. Chernov).

0022-3115/$ - see front matter © 2007 Elsevier B.V. All rights reserved.
doi:10.1016/j.jnucmat.2007.03.134

SPDs in stable, metastable and saddle point configurations were calculated in [3,4]. Interatomic interactions in model crystallites were described by an interaction potential from [5] for BCC Fe and by EAM-type interaction potential from [6] for FCC Cu. Table 1 lists calculated characteristics of SPDs in Fe and Cu. Comparison of the characteristics of SPDs presented here in the absence of the stresses with experimental data was conducted in [3,6] and demonstrated good agreement.

The stable SIA configurations are the $\langle 1\,1\,0\rangle$ dumbbell in Fe and the $\langle 1\,0\,0\rangle$ dumbbell in Cu. The $\langle 1\,1\,0\rangle$ and $\langle 1\,0\,0\rangle$ dumbbells jump to the nearest lattice sites with a 60° and 90° rotation of the dumbbell axis, respectively. This is the SIA migration mechanism with the lowest migration energy, 0.25 eV and 0.10 eV, in Fe and Cu. The elastic dipole corresponding to the saddle point configuration of the $\langle 1\,1\,0\rangle$ and $\langle 1\,0\,0\rangle$ dumbbells has 12 (monoclinic symmetry) and 6 (orthorhombic symmetry) possible equivalent orientations, respectively (Table 1).

The elastic dipole corresponding to the vacancy saddle point configuration has four possible equivalent orientations (trigonal symmetry) in Fe and six (orthorhombic symmetry) in Cu (Table 1). The vacancy migration energy is equal to 0.735 eV and 0.69 eV in Fe and Cu, respectively.

3. Elastic stress fields of dislocations

Stress fields, σ_{ij}^{d}, of straight perfect edge dislocations in slip systems $\langle 1\,1\,1\rangle\{1\,1\,0\}$ (Burgers vector $\boldsymbol{b} = a/2[1\,1\,1]$) and $\langle 1\,0\,0\rangle\{1\,0\,0\}$ ($\boldsymbol{b} = a[1\,0\,0]$) in Fe and $\langle 1\,1\,0\rangle\{1\,1\,1\}$ ($\boldsymbol{b} = a/2[1\,1\,0]$) in Cu were calculated within the anisotropic linear theory of elasticity, following an algebraic method [2]. Elastic constants C_{11}, C_{12}, C_{44} and lattice constants a used for calculation of dislocation stress fields are in accord with values provided the interatomic potential used: $C_{11} = 243.1$ GPa, $C_{12} = 138.1$ GPa, $C_{44} = 121.9$ GPa, $a = 0.28665$ nm for Fe; $C_{11} = 169.9$ GPa, $C_{12} = 122.6$ GPa, $C_{44} = 76.2$ GPa, $a = 0.3615$ nm for Cu.

4. Interaction of dislocations with SPDs

The formation energy $E_{\mathrm{d}}^{\mathrm{F}}$ of a point defect in the neighborhood of a dislocation can be written as

$$E_{\mathrm{d}}^{\mathrm{F}}(\boldsymbol{r}) = E^{\mathrm{F}} + E_{\mathrm{int}}(\boldsymbol{r}), \tag{1}$$

where E^{F} is the formation energy of the point defect in the absence of the dislocation, $\boldsymbol{r}$ is the radius-vector of the position of the point defect with respect to the dislocation and E_{int} is the interaction energy between the dislocation and the point defect.

Table 1
Calculated formation energies E^{F} (in eV), relaxation volumes V^{R} (in atomic volumes) and dipole tensors P_{ij} (in eV) of self-point defects in BCC Fe and FCC Cu in the absence of dislocation stress fields (N is the number of possible crystallographic orientations for the considered elastic dipoles) [3,4]

Material	Self-point defect	E^{F}[a]	V^{R}	P_{11}	P_{22}	P_{33}	P_{13}	P_{23}	P_{12}	N[b]
Fe	$\langle 1\,1\,0\rangle$ dumbbell	4.384	1.480	18.04	18.04	20.39	0	0	4.99	6
	$\langle 1\,1\,0\rangle$ dumbbell saddle point	4.630	1.476	18.88	18.57	18.88	3.26	5.16	5.16	12
	$\langle 1\,1\,1\rangle$ dumbbell	4.627	1.436	18.27	18.27	18.27	6.37	6.37	6.37	4
	Crowdion	4.635	1.442	18.35	18.35	18.35	6.32	6.32	6.32	4
	Tetrahedral	5.149	1.286	15.60	16.74	16.74	0	0	0	3
	Octahedral	5.464	1.174	21.02	11.89	11.89	0	0	0	3
	$\langle 1\,0\,0\rangle$ dumbbell	5.618	1.171	19.86	12.41	12.41	0	0	0	3
	Vacancy	1.920	−0.140	−1.78	−1.78	−1.78	0	0	0	1
	Vacancy saddle point	2.655	−0.112	−1.43	−1.43	−1.43	−1.68	−1.68	−1.68	4
Cu	$\langle 1\,0\,0\rangle$ dumbbell	3.068	1.848	18.55	18.99	18.99	0	0	0	3
	$\langle 1\,0\,0\rangle$ dumbbell saddle point	3.166	1.887	19.09	19.09	19.57	0	0	2.22	6
	Octahedral	3.243	1.902	19.40	19.40	19.40	0	0	0	1
	$\langle 1\,1\,0\rangle$ dumbbell	3.302	1.906	18.38	18.38	21.57	0	0	10.48	6
	Crowdion	3.303	1.904	18.36	18.36	21.55	0	0	10.46	6
	$\langle 1\,1\,1\rangle$ dumbbell	3.504	1.945	19.84	19.84	19.84	3.53	3.53	3.53	4
	Tetrahedral	3.553	1.959	19.98	19.98	19.98	0	0	0	1
	Vacancy	1.272	−0.298	−3.04	−3.04	−3.04	0	0	0	1
	Vacancy saddle point	1.962	−0.189	−3.72	−3.72	1.66	0	0	−0.76	6

[a] The values of the self-point defect formation energies presented in Table 2 of [5] are incorrect.
[b] $N = 1, 3, 4, 6, 12$ corresponds to cubic, tetragonal, trigonal, orthorhombic, monoclinic symmetries of point defect configuration, respectively.

The interaction energy E_{int} within the framework of the linear theory of elasticity is given by [1,7–9]

$$E_{\text{int}}(\boldsymbol{r}) = E_{\text{int}}(r,\varphi) = -P_{ij}\varepsilon^{\text{d}}_{ij}(\boldsymbol{r}) = -P_{ij}S_{ijkl}\sigma^{\text{d}}_{kl}(\boldsymbol{r}), \quad (2)$$

where r is the distance between the point defect (elastic dipole) and the dislocation, φ is the angle between $\boldsymbol{r}$ and $\boldsymbol{b}$, S_{ijkl} is the elastic compliance tensor and $\varepsilon^{\text{d}}_{ij}$ is the elastic strain tensor caused by a dislocation. At distances less than $\sim a$, it is necessary to use additionally atomistic models ([3,10,11]) to check the validity of the linear approximation.

Dislocation stress fields eliminate degeneracy of the formation energies of crystallographically equivalent different orientations of SPDs. This can result in: (1) change of the most energetically favorable SIA configuration near the dislocation, and (2) anisotropic migration of SPDs.

4.1. Change of stable SIA configuration in the neighborhood of dislocations

Near a $\langle 1\,1\,1\rangle\{1\,1\,0\}$ dislocation in Fe, the formation energy of a $\langle 1\,1\,1\rangle$ dumbbell is less than the formation energy of a $\langle 1\,1\,0\rangle$ dumbbell. Fig. 1(a) shows the region of stabilization of a $\langle 1\,1\,1\rangle$ dumbbell and spatial dependence of the most energetically favorable $\langle 1\,1\,1\rangle$ dumbbell orientations. In the angle range $7° < \varphi < 173°$, the most energetically preferable SIA configuration is a $\langle 1\,1\,1\rangle$ dumbbell with the axis parallel to the Burgers vector orientation. The $\langle 1\,1\,1\rangle$ dumbbell formation energy maximum at $\varphi = 90°$ is located between two minimums at angles of $\varphi = 70°$ and $\varphi = 110°$. In the specified angle range, a $\langle 1\,1\,1\rangle$ dumbbell has to change its orientation to the energetically unfavourable one to get closer to the dislocation. Therefore, $\langle 1\,1\,1\rangle\{1\,1\,0\}$ dislocation stress fields make a field-effect trap for $\langle 1\,1\,1\rangle$ dumbbell, which makes its approach to the dislocation core difficult. This result is in agreement with the results of the molecular dynamics study [12]. The stabilization region of a $\langle 1\,1\,1\rangle$ dumbbell is absent in the neighborhood of a $\langle 1\,0\,0\rangle\{1\,0\,0\}$ dislocation in Fe.

In the neighborhood of a $\langle 1\,1\,0\rangle\{1\,1\,1\}$ dislocation in Cu, the formation energy of a $\langle 1\,1\,0\rangle$ dumbbell is less than the formation energy of a $\langle 1\,0\,0\rangle$ dumbbell. Fig. 1(b) shows the region of stabilization of a $\langle 1\,1\,0\rangle$ dumbbell and the spatial dependence of the most energetically favorable $\langle 1\,1\,0\rangle$ dumbbell orientations. In the angle ranges $-11° < \varphi < 82°$ and $98° < \varphi < 191°$ the most energetically preferable SIA configuration is a $\langle 1\,1\,0\rangle$ dumbbell with the axis parallel to the slip plane orientation. $\langle 1\,1\,0\rangle$ dumbbell formation energy minimums are located at angles $\varphi = 40°$ and $\varphi = 140°$. In the specified angle ranges, a $\langle 1\,1\,0\rangle$ dumbbell has to change its orientation to the energetically unfavourable one to get closer to the dislocation core. Therefore, $\langle 1\,1\,1\rangle\{1\,1\,0\}$ dislocation

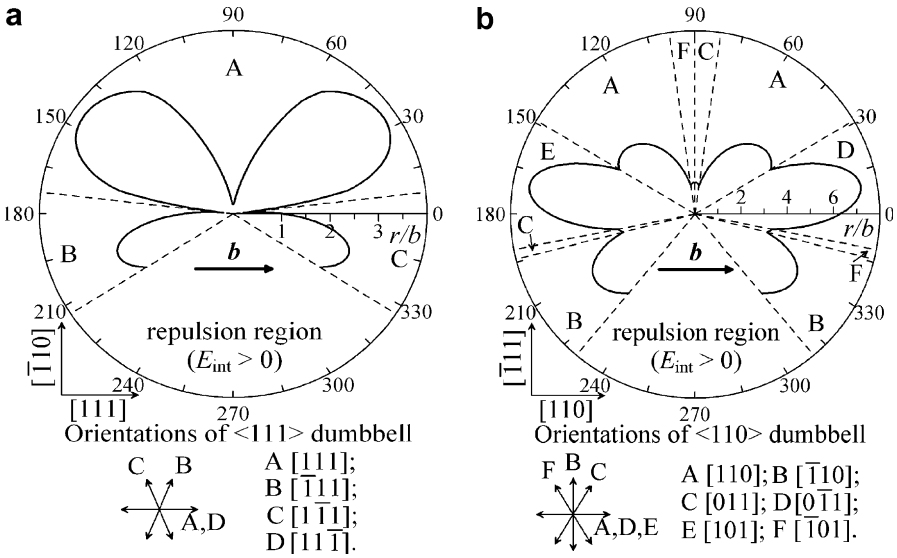

Fig. 1. Spatial regions of stabilization for SIA configurations in the neighborhood of dislocations (dotted lines demarcate the regions with different energetically favorable orientations of the self interstitial). (a) $\langle 1\,1\,1\rangle$ dumbbell, $\langle 1\,1\,1\rangle\{1\,1\,0\}$ dislocation, Fe; (b) $\langle 1\,1\,0\rangle$ dumbbell, $\langle 1\,1\,0\rangle\{1\,1\,1\}$ dislocation, Cu.

stress fields make a field-effect trap for ⟨1 1 0⟩ dumbbell, which makes its approach to the dislocation core difficult. However, in the angle range $82° < \varphi < 98°$ the most energetically preferable ⟨1 1 0⟩ dumbbell orientations are directed toward the dislocation core.

4.2. Migration of SPDs in the neighborhood of dislocations

Each orientation of an elastic dipole relative to a point defect saddle point configuration corresponds to a certain migration direction. Using Eqs. (1) and (2) to calculate the formation energies of all possible orientations of the defect saddle point configuration at some point $\boldsymbol{r}$, we can determine the point defect migration direction with the lowest migration energy at this point and plot migration pathways along which the migration of the point defect has the lowest energy barriers.

To characterize distances at which anisotropic migration becomes significant, we calculated average distances $\bar{r}$ (Table 2) to the dislocations, at which difference between migration energies of the SPDs in different directions is larger than value of $k_B T$ (k_B is Boltzmann's constant) at $T = 293$ K. $\bar{r}$ for SIA is three times as large as $\bar{r}$ for vacancy in Fe. However, $\bar{r}$ for SIA is half as large as $\bar{r}$ for vacancy in Cu. These features are the consequence of highly anisotropic dipole tensors for saddle point configurations of the ⟨1 1 0⟩ dumbbell in Fe and vacancy in Cu and relatively low anisotropy for saddle point configurations of the ⟨1 0 0⟩ dumbbell in Cu and vacancy in Fe (Table 1).

4.2.1. ⟨1 1 1⟩{1 1 0} dislocation in Fe

For the ⟨1 1 0⟩ dumbbell attractive region, the pathways are parallel to the slip plane, which makes it difficult for the SIA to approach the dislocation (Fig. 2(a)). Besides, in the neighborhood of the dislocation, the SIA falls into the field-effect trap mentioned above.

Table 2
Average distance $\bar{r}$ to the dislocations, at which difference between migration energies of the self-point defects in different directions is larger than the value of $k_B T$ at $T = 293$ K

Material	Dislocation	$\bar{r}$ (b)	
		SIA	Vacancy
Fe	⟨1 1 1⟩{1 1 0}	60	19
	⟨1 0 0⟩{0 0 1}	30	9
Cu	⟨1 1 0⟩{1 1 1}	16	28

In the vacancy attractive region in the angle range $233° < \varphi < 307°$, the migration directions with the lowest migration energy are parallel to the Burgers vector and directed outwards from the dislocation which makes it difficult for it to approach the dislocation (Fig. 2(b)).

4.2.2. ⟨1 0 0⟩{1 0 0} dislocation in Fe

In the angle range $-39° < \varphi < 219°$ (Fig. 2(c)), the migration directions of a ⟨1 1 0⟩ dumbbell with the lowest migration energy are directed towards the dislocation. The stabilization region of a ⟨1 1 1⟩ dumbbell is absent, so the SIA can fall into the dislocation core without difficulties.

In the angle range $260° < \varphi < 280°$ (Fig. 2(d)), the migration directions of a vacancy with the lowest migration energy are directed outwards from the dislocation which makes it difficult for it to approach the dislocation.

4.2.3. ⟨1 1 0⟩{1 1 1} dislocation in Cu

In the ⟨1 0 0⟩ dumbbell attraction region, the pathways are parallel to the dislocation slip plane with the exception of the angle range $82° < \varphi < 98°$ (Fig. 2(e)). In this region the migration directions of a ⟨1 0 0⟩ dumbbell with the lowest migration energies are directed to the dislocation. Thus, the pathways of an SIA with the lowest energy barriers move around the field-effect trap mentioned above because of the change of the most stable SIA configuration near the dislocation.

In the angle ranges $218° < \varphi < 245°$, $262° < \varphi < 278°$, $295° < \varphi < 322°$ (Fig. 2(f)), the migration directions of a vacancy with the lowest migration energy are directed outwards from the dislocation which makes it difficult for it to approach the dislocation.

5. Conclusion

1. Interaction energies of SPDs (elastic dipoles) with edge dislocations in slip systems ⟨1 1 1⟩{1 1 0} and ⟨1 0 0⟩{1 0 0} in BCC Fe and ⟨1 1 0⟩{1 1 1} in FCC Cu were calculated by methods of the anisotropic theory of elasticity and molecular statics (hybrid method).
2. Crystallographic characteristics of SPDs and edge dislocations significantly effect the migration energies of SPDs in dislocation stress fields.
3. ⟨1 1 0⟩ dumbbell jumps with the lowest migration energy are directed parallel to the Burgers vector in the attractive region of an SIA with a ⟨1 1 1⟩{1 1 0} dislocation in Fe. Dislocation stress

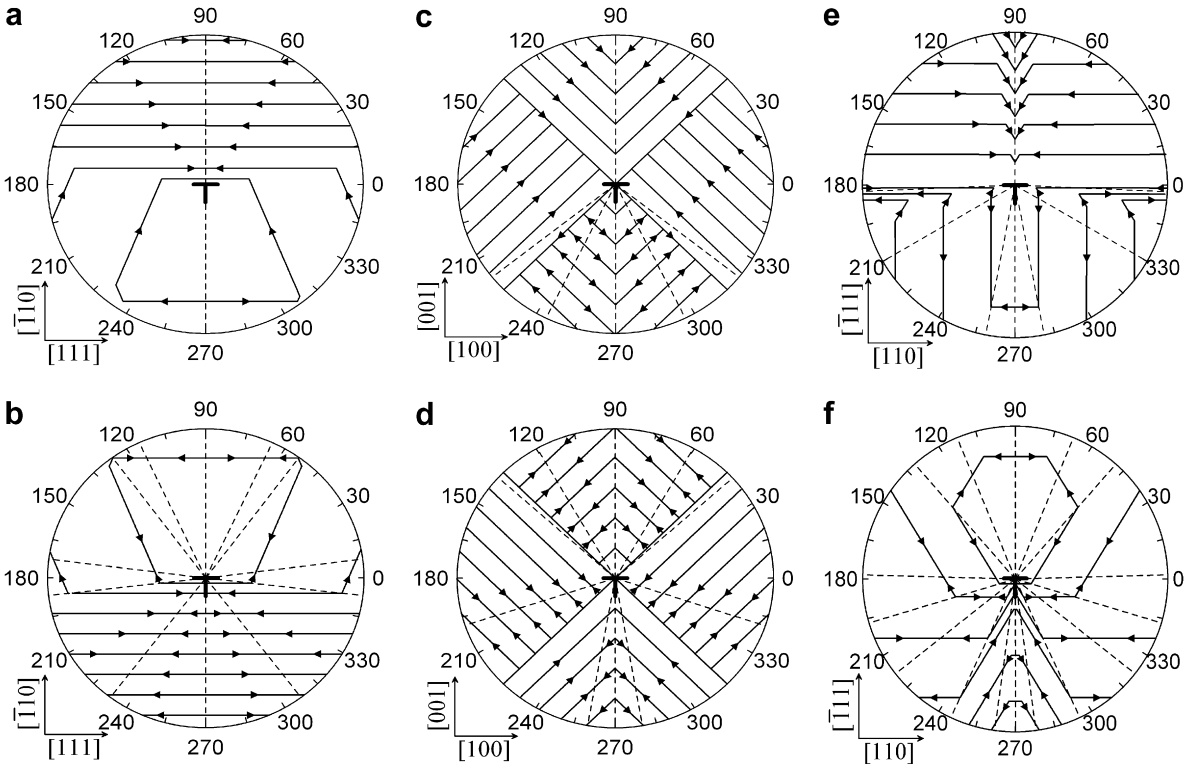

Fig. 2. Migration pathways of the self-point defects with the lowest energy barriers in dislocation stress fields (arrows show the direction of the self-point defect motion along the pathway; dotted lines are rays $\varphi = \text{const.}$ corresponding to turning points in the defect migration along the pathway). (a) $\langle 110\rangle$ dumbbell, $\langle 111\rangle\{110\}$ dislocation, Fe; (b) vacancy, $\langle 111\rangle\{110\}$ dislocation, Fe; (c) $\langle 110\rangle$ dumbbell, $\langle 100\rangle\{100\}$ dislocation, Fe; (d) vacancy, $\langle 100\rangle\{100\}$ dislocation, Fe; (e) $\langle 100\rangle$ dumbbell, $\langle 110\rangle\{111\}$ dislocation, Cu; (f) vacancy, $\langle 110\rangle\{111\}$ dislocation, Cu.

fields stabilize the $\langle 111\rangle$ dumbbell configuration of an SIA oriented parallel to the Burgers vector, which also impedes SIA approach to the dislocation.

4. In the neighbourhood of $\langle 100\rangle\{100\}$ dislocation in Fe, the region of stabilization of the $\langle 111\rangle$ dumbbell is absent, and the migration directions of a $\langle 110\rangle$ dumbbell with the lowest migration energy are directed towards the dislocation.
5. A $\langle 100\rangle$ dumbbell can migrate to the $\langle 110\rangle\{111\}$ dislocation core in Cu without difficulties since the pathways of an SIA with the lowest energy barriers move around the field-effect trap concerned with the stabilization of a $\langle 110\rangle$ dumbbell oriented parallel to the Burgers vector near the dislocation.
6. Vacancy migration to the considered dislocations is impeded since the migration directions of a vacancy with the lowest migration energy are directed outwards from the dislocation.
7. Average distance to the dislocations, at which difference between migration energies of the SPDs in different directions is larger than value of $k_B T$ at $T = 293$ K, equals $\sim 30b$ and may significantly vary depending on the dislocation type and SPD configuration.
8. Indicated features of SPDs behavior in dislocation fields can exert a significant influence on the efficiency of the dislocations as sinks for SPDs in crystals with different symmetries and, consequently, on evolution of material microstructure under damage irradiation (swelling, creep, etc).

Acknowledgement

The present work was funded by Russian Foundation for Basic Research (project RFBR 05-02-08128ofi-e).

References

[1] V.L. Indenbom, J. Lothe (Eds.), Elastic Strain Fields and Dislocation Mobility, North-Holland, Amsterdam, 1992.

[2] J.P. Hirth, J. Lothe, Theory of Dislocations, McGraw-Hill, New York, 1968.
[3] V.A. Romanov, A.B. Sivak, V.M. Chernov, Voprosy Atomnoi Nauki i Tekhniki Ser. Materialovedenie i novye materialy 1 (66) (2006) 129, in Russian.
[4] N.A. Dubasova, A.B. Sivak, V.M. Chernov, Voprosy Atomnoi Nauki i Tekhniki Ser. Materialovedenie i novye materialy 1 (66) (2006) 233, in Russian.
[5] A.B. Sivak, V.A. Romanov, V.M. Chernov, J. Nucl. Mater. 323 (2003) 380.
[6] Y. Mishin, M.J. Mehl, D.A. Papaconstantopoulos, A.F. Voter, J.D. Kress, Phys. Rev. B 63 (2001) 224106.
[7] J.D. Eshelby, in: F. Seitz, D. Turnball (Eds.), Solid State Physics, vol. 3, Academic Press, New York, 1956, p. 79.
[8] E. Kröner, Kontinuumstheorie der Versetzungen und Eigenspannungen, Springer, Berlin – Göttingen – Heidelberg, 1958.
[9] M.P. Puls, C.H. Woo, J. Nucl. Mater. 139 (1986) 48.
[10] E. Kuramoto, K. Ohsawa, T. Tsutsumi, J. Nucl. Mater. 283–287 (2000) 778.
[11] Yu.N. Osetsky, D.J. Bacon, F. Gao, A. Serra, B.N. Singh, J. Nucl. Mater. 283–287 (2000) 784.
[12] H. Kamiyama, H. Rafii-Tabar, Y. Kawazoe, H. Matsui, J. Nucl. Mater. 212–215 (1994) 231.